# The Pandemic Holiday Blip in New York City

Maximilian Vierlboeck, Roshanak Rose Nilchiani, and Christine M. Edwards, *Member, IEEE*

*Abstract*—When it comes to pandemics, such as the one caused by the Coronavirus disease COVID-19, various issues and problems have arisen for the healthcare infrastructure and institutions. With increasing number of patients in need of urgent medical care and hospitalizations, the healthcare systems and regional hospitals may approach their maximum service capacity and may face shortage of various parameters, such as supplies including PPE, medications, therapeutic devices, ventilators, beds, and many more. The article at hand describes the development and framework of a simulation model that enables the modeling and evaluation of the COVID-19 pandemic progress. To achieve this, the model dynamically mimics and simulates the developments and time-dependent behavior of various crucial parameters of the pandemic, among others, the daily infection numbers and death rate. In addition, the model enables the simulation of single events and scenarios that occur outside of the regular pandemic developments as anomalies, such as holidays. Unlike traditional models, the proposed framework is based on factors and parameters closely derived from reality, such as the contact rate of individuals, which allows for a much more realistic representation. In addition, the real connection enables the assessment of effects of various influences regarding the development and progress of the pandemic, such as hospitalization numbers over time. All the aforementioned points are possible within the simulation framework and do not require awaiting the unfolding of the effects in reality. Thus, the model is capable of dynamically predicting how different scenarios turn out. The abilities of the model are demonstrated, illustrated, and proven in a specific case study that shows the impact of holidays, such as Passover and Easter in New York City when quarantine measures might have been ignored, and an increase in extended family gatherings temporarily occurred. As a result, the simulation showed significant impacts and disproportionate number of patients in need of medical care that could be potentially detrimental in reality. For example, compared to the previous trajectory of the pandemic, for a temporary increase of 50% in the contact rate of individuals, the model showed that the total number of cases would increase by 461 090, the maximum number of required hospitalizations would rise to 79 733, and the total number of fatalities would climb by 19 125 over 90 days. In addition to its function and proven capabilities, the model can and is furthermore planned to be adapted to other areas, not necessarily only metropolitan regions in order to expand the utilization of its predictive power. Such predictions could be used to derive regulatory measures and to test various policies for COVID-19 containment.

*Index Terms*—Adaptability, complex system modeling, contact rate, COVID-19, dynamic simulation, hospitalization, pandemic, SARS-CoV-2.

## I. Introduction, Situation, and Problem

"A PANDEMIC is the worldwide spread of a new disease" [1]. This definition by the WHO describes the current global situation of COVID-19 [2] that emerged worldwide in early 2020. The virus is confirmed to be transmissible from human to human [3], [4] and has constantly been spreading due to contact between individuals.

Although it may appear as if the spread of COVID-19 is following a simple exponential mathematical model, it is dynamic, complex, and nonlinear. Therefore, predictions can be difficult and the actual behavior of the system and the outcome, such as fatalities and healthcare infrastructure strain, can be hard to evaluate. One way to enable evaluations is to design a representative system dynamics model that simulates the real-world phenomena as precisely as possible. With such a model, certain parameters and influences can be assessed by changing input parameters and observing the results and model reactions, which is what this article addresses.

Due to the importance of transmission from human to human and the involved contact, the research presented focuses on the actual contact rate between humans in a dynamic simulation using New York City as an example, in order to determine which factors play a critical role and how certain influences interact. Therefore, various scenarios were assessed in order to observe different behaviors and discover potential emergent phenomena of the system and model.

Section II describes the current state of the research and other relevant approaches, in relation to the work at hand. Section III describes the research methodology, the model utilized for the simulations, and how the specific simulations were conducted. Subsequently, Section IV provides the assumptions that were made in order to design and set up the model as well as the involved parameter. Sections V and VI demonstrate scenarios that are possible and likely to occur in order to show the behavior of the system and discovered emergent phenomena. Section VII summarizes and discusses the outcomes and last, Section VIII gives a comprehensive conclusion for the presented work.

## II. Current State of the Research and Literature

Since the onset of the pandemic at the beginning of the year 2020, there have been several articles and publications that address and scientifically approach the spread of the COVID-19 disease. In order to define the state of the research and current work, literature research was conducted. The results of this review are summarized hereinafter.

In order to simplify the overview, groups of similar research publications and approaches have been conflated and are listed below.

The first group comprises approaches that utilize machine learning and artificial intelligence to model and predict the

spread of the disease [5]–[8]. These approaches are based on underlying algorithms, such as adaptive network-based inference systems, and can yield predictions for various time periods due to a low dependence on sample data as input. Yet, the utilized algorithms and types, thereof, critically define and shape the progress and in the case of the machine learning approaches, accuracy can also increase with longer application duration. Such approaches provide a flexible way to predict and / or analyze the progress of a pandemic. However, they are strongly dependent on the specific methodologies and / or algorithms utilized, since these components shape the results and behavior.

The second group of models relies solely on statistical measures and the respective mathematical tools to predict and evaluate the progress of the pandemic on an iterative basis without reliance on simulation [9]–[12]. Due to the mathematical foundations underlying these approaches, such as average and trend evaluation, monitoring is enabled and even allows for a continuous evaluation as new data can be included right away for iterative predictions. Yet, such methods are difficult to use without data to rely on or scenarios to evaluate.

The third group utilizes simulations of various types, also partially in combination with the previous group based on mathematical tools. The publications describing simulations [13]–[15] show the possibility to evaluate scenarios, but due to their underlying equations and foundations, they also deviate from reality as they simulate the progress iteratively and sequentially instead of mirroring real parameters.

Last, there are other research efforts regarding passive influencing factors that are environmental in nature, such as seasonal influences and measures that affect the disease spread [16], [17]. These publications provide a similar predictive power compared to the work at hand, but they differ as their assessments are mostly focusing on the progress of the pandemic in a general sense and implement the mentioned influences as modulating factors for the transmission, rather than forming causal connections that can be or become nonlinear and or dynamic.

The next section outlines the developed model based on the direct representation and inclusion of real parameters, such as the contact rate. Subsequently, the application of the model is described for various scenarios including the results and implications thereof.

## III. MODEL AND METHODOLOGY

When looking at various models for the spread of diseases, SIR models present a simple and easy to adapt starting point for such situations. SIR stands for "susceptible–infective–removed" and was first proposed by Kermack and McKendrick in 1927 [18]. The model is described as a differential system in which multiple factors depend on each other to determine the behavior of the three stocks $S$, $I$, and $R$. In such a setup, simulated individuals process through the model from "susceptible" to "infective" and then to "removed," without the option to return to a previous stage at any point. The rates at which individuals are transferred from one stage to the other are defined by the transition parameters. The

parameter $\beta$, which defines the transition from $S$ to $I$, depends on the ratio of infected to susceptible people, as well as an infection probability parameter of the disease. The parameter $\gamma$, describing the transitions from $I$ to $R$, is defined by the likelihood of an individual recovering and thus being removed from the infectious stock. The total number of individuals in the simulation does, herein, not change over time and is equal to $N$, which therefore forms the sum of all stocks at all times.

Thus, the equations of an SIR model are as follows [19]:

Susceptible Population:
$$\dot{S} = -\beta S \quad \text{with} \quad S(0) = S_o \geq 0 \qquad (1)$$

Infectious Population:
$$\dot{I} = \beta S - \gamma I \quad \text{with} \quad I(0) = I_o \geq 0 \qquad (2)$$

Removed Population:
$$\dot{R} = \gamma I \quad \text{with} \quad R(0) = R_o \geq 0 \qquad (3)$$

so that $S(t) + I(t) + R(t) = N$ and $\dot{S} + \dot{I} + \dot{R} = 0$.

With these equations, a simulation system was derived that models the situation of the COVID-19 pandemic and spread. Since the healthcare infrastructure, resources, and personnel are of importance for the COVID-19 management and mitigation, the model includes time delays due to incubation and a portion of the infected people that do not go directly from "infected" to "removed," but rather move to hospitalization. From hospitalization then, there are two possible paths, either a delayed demise of the individual, or a delayed recovery, which adds the individual to the stock of $R$. The stock of $R$ is final, which means that for the framework presented, individuals cannot return to the susceptible stock and are thus assumed to be immune to COVID-19 for the duration of the simulation.

The mentioned delays were implemented as timed delays, meaning that a certain amount of time had to pass before the transition of an individual would occur. This was implemented by dividing the respective transition rate by the delay in time steps. All delays were deduced from official reports and guidelines at the time of the creation [20]–[25] and can be updated as well as adapted to different surroundings and circumstances.

All of the above described additions modify the equations as follows and amend (7) and (8):

Susceptible Population:
$$\dot{S} = -\beta S \quad \text{with} \quad S(0) = S_o \geq 0 \qquad (4)$$

Infectious Population:
$$\dot{I} = \beta S - \gamma I - \lambda I \quad \text{with} \quad I(0) = I_o \geq 0 \qquad (5)$$

Removed Population (delayed recovery [20], [21], [25]):
$$\dot{R} = \gamma I + \alpha H \quad \text{with} \quad R(0) = R_o \geq 0 \qquad (6)$$

Hospitalized Population (incubation delay [20], [22]–[24]):
$$\dot{H} = \lambda I - \delta H - \alpha H \quad \text{with} \quad R(0) = R_o \geq 0 \quad (7)$$

Deceased Population (delayed by mortality [20], [24]):
$$\dot{D} = \delta H \quad \text{with} \quad R(0) = R_o \geq 0 \qquad (8)$$
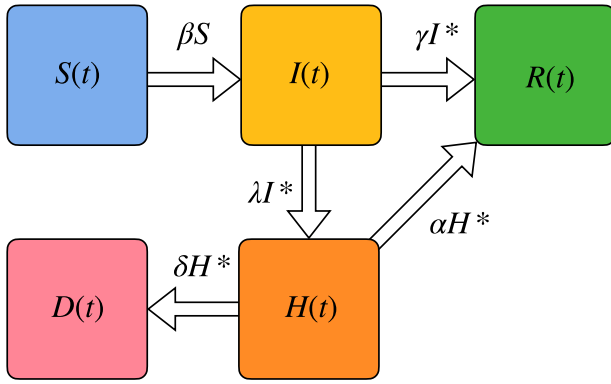
Fig. 1. Simulation Flowchart (∗ marks delay impacts). The full simulation model and structure can be provided upon request.

so that $S(t) + I(t) + R(t) + H(t) + D(t) = N$ and $\dot{S} + \dot{I} + \dot{R} + \dot{H} + \dot{D} = 0$.

A flowchart of the implementation is shown in Fig. 1 on the right as a direct representation of (4)–(8). The rates and parameters are each implemented and color-coded accordingly in the equations.

The actual simulation based on these parameters was setup in Vensim [26] with time and calculation steps of one day. Vensim [26] is a simulation software developed and distributed by Ventana Systems. The software allows for the creation of continuous simulation models that enable, amongst other aspects, the assessment of dynamic system behaviors. The base parameter of a Vensim simulation framework, besides the flows and stocks described below in more detail, is the step and progress of the simulation. Based on the defined steps, the simulation progresses dynamically within a set time frame. These steps were set as one day in the presented framework and were simulated for time periods of 90 days. Thus, the simulation completes the transitions and process steps once "per day" for 90 days iteratively, using the previous step as input and creating a new step as output.

In addition to the time-related framework, Vensim allows for the modeling of stocks that represent and visualize the behavior and changes of certain groups in the simulation. These stocks were defined and created in accordance with (4)–(8). Thus, the changes and dynamics of all stocks could be evaluated over the given time period for various simulation runs and scenarios.

Based on the equations and the structure shown in Fig. 1, the model was created, which is further described in Section IV. A complete schematic overview of the Vensim simulation model structure and the respective source files can be provided upon request. The model was designed in order to allow for a flexible adjustment of the parameters, which is described in Section IV (see Fig. 1). The chosen research methodology was applied as described by Maria [27]. Herein, after the problem definition in the first step, the parameters of the model were set to yield an adequate and verifiable outcome. This verification was conducted by comparing the model results to real-world data that was reported and recorded during the pandemic.

With the set parameters (also see Section IV), multiple scenarios were simulated and examined based on various conditions that were chosen, derived from real and current circumstances. These scenarios are described in Sections V and VI.

The scenarios were then assessed for the phenomenon the authors called the "Pandemic Holiday Blip" (Section VI). Based on the results, predictions of possible behaviors of the current pandemic were deduced to potentially support governing and regulating decisions, in order to avoid and mitigate unwanted situations, such as high fatality numbers or the collapse of medical support.

Section IV describes the assumptions made for the model to allow for simulations that mimic the current real-world behavior as far as possible.

## IV. ASSUMPTIONS AND PARAMETER

In order to design a model that could mimic and simulate the COVID-19 pandemic, the factors described in (4)–(8) had to be set so that the simulation results would be in accordance with real-world situations and data. Therefore, this section outlines the assumptions that were made in order to achieve the accordance. Hence, the following subsections describe each parameter individually based on New York City (NYC) in 2020, with a total population of 8.4 million people [28].

### A. Parameter β-Infection Rate

The infection rate of the model, which describes at what rate the susceptible population is infected, was defined depending on two factors: infectivity $i$ and contact rate $c$. These two factors, together with the infectious population ($I$) and the susceptible population ($S$), allow for the calculation of the infection rate according to the following formula:

$$\beta \cdot S = c \cdot S(t) \cdot \frac{I(t)}{N - D(t)} \cdot i.$$

The infectivity $i$ was defined as a constant based on the likelihood of infection when people interact and hence was derived from various sources and set to 5% [29], [30], due to the higher population density of NYC compared to the locations of the source data. The constant infectivity allowed a modulation and adjustment of the infection rate based on the second component: the contact rate. This rate was furthermore used to model and simulate policies such as social distancing and their impact on the contact rate of the population. For the general magnitude of the contact rate, the number of average contacts of people per day in NYC was researched in order to enable a realistic starting point without any measures.

Based on the literature sources, the researched contact rate in NYC ranged from five for people who do not use the subway, up to at least ten for people who do utilize the subway [31]. Since these data were obtained and measured in 2003 and the population of NYC increased by 5% since then, today's contact rates are 5.25 and 12.5, respectively. Given that the number of subway users in NYC is higher than in any other city in the United States [32], it was assumed that 70% of the NYC population take the subway on a daily basis and thus effectively have more contacts, including indirect exposures

through surfaces and objects. Together with the number of contacts for nonsubway users, this yields an average contact rate without restrictions or social distancing of 10.325 for NYC.

With these factors, the infection rate was defined by the following equation:

$$\beta \cdot S = c(t) \cdot S(t) \cdot \frac{I(t)}{N - D(t)} \cdot i$$

with

$$c_0 = 10.325.$$

### B. Parameters $\gamma$ and $\lambda$—Recovery and Hospitalization Rate

The parameters for the hospitalization and recovery rate were assumed to be directly connected as an infected person would either recover or be hospitalized (see Fig. 1). Hence, the recovery rate is the opposite portion of the hospitalization rate

$$\gamma + \lambda = 1.$$

Since the numbers of hospitalizations vary by age group and therefore depend on demographics, an average hospitalization rate was calculated based on official data by the City of New York [33] in combination with demographics to allow for the use of a constant. The resulting probability was 0.27 for hospitalization and 0.73 for recovery

$$\gamma = 0.27 \text{ and } \lambda = 0.73.$$

### C. Parameters $\alpha$ and $\delta$—Hospital Recovery and Mortality

Similar to the last subsection, the parameters for the hospital recovery and death rate were also assumed directly connected, as a hospitalized person would either recover or decease. Therefore, the hospital recovery rate was the opposite portion of the death rate, yielding

$$\alpha + \delta = 1.$$

Since the death rate for people hospitalized is much higher than the death rate caused by the virus in general, the death rate after hospitalization was calculated based on the number of confirmed deaths and hospitalizations provided by the City of New York [33], which resulted in a death rate of 0.223 and a hospital recovery rate of 0.777

$$\alpha = 0.777 \text{ and } \delta = 0.223.$$

### D. Final Assumptions and Unknown Numbers

The first positive COVID-19 case was reported in New York City on March 1. Unfortunately, this is only the first confirmed positive case and not necessarily or likely the first case of the city in general. Throughout the spread of the virus, only cases tested positive were reported which causes a lack of statistics on silent carriers/transmitters of the COVID-19 virus [34]. Thus, the number of COVID-19 cases resulting from a simulation will be higher than what the official positive COVID-19 test data represent. Actual numbers and estimation for the unknown numbers are hard to find and estimates range from over 70% unknown cases [35] to ten times the confirmed number or more [36]. Therefore, the number of unknown cases

in the model was adjusted so that the model aligned from March 1 to 20 with the reported real time data. In order to achieve this, the model was set to 15 infections at the time of the first reported case. This leads to a realistic outcome of the simulation and serves as verification of the design, as the fatality rate and the case numbers correlate with the data when taking into consideration the unknown case numbers (see Scenarios I and II for verification).

As mentioned above, the total population of this case study in NYC region was utilized as a single constant number. In reality, such a number can fluctuate due to births, natural deaths, migration, and other factors. Thus, these factors would have to be included in the simulation and they could potentially affect the outcome. Yet, these factors were omitted for this simulation and the assessed scenarios due to two reasons. The first reason is the short time frame of the simulation, which is limited to 90 days only. In such a short time span, the effect of deaths not related to COVID-19 can be seen as a negligible amount that would not even exceed 0.25% of the population of the NYC area [37]. Furthermore, if births are taken into account, the fluctuation for a 90-day period can be considered entirely negligible since it is under 0.1% [38]. The second reason is the fact that during the evaluated time, various migration inhibiting measures were put in place, such as border closures. Due to these measures, in combination with assessed mobility data [39], the effect of migration during the evaluated time was deemed negligible as well.

With these settings and parameters, the scenarios for the simulation could be run and evaluated by modulating the contact rate based on various possible changes and adjustments. Since the measures and regulations that were put into place are hard to quantify, the first scenarios address the effects of such measures and show how they could have affected the numbers. Then, the ensuing scenarios evaluate possible occurrences and events. Section V covers these scenarios and discusses the general effects of the variable in the simulation: the contact rate. Section VII discusses the results further and shows a possible phenomenon.

## V. Baseline Scenarios and General Effects

As described above, the purpose of the first baseline scenario was to create the trajectory of COVID-19 cases over the period of three months that follows the reported data. As mentioned, the variable utilized to modulate and therefore manipulate the simulation is the contact rate which directly affects the infection rate. This connection stems from the fact that the infection rate is driven by the infectivity, which is assumed constant for the virus, in multiplication with the contact rate (see parameter $\beta$).

### A. Scenario 1—Immediate Social Distancing and Closure of Offices and Businesses

The first measure put in place in NYC was social distancing, and the immediate closure of certain institutions, businesses, and stores. This was accompanied by companies transitioning employees to work from home or stopping work all together. Official orders went into place on March 16 and March 21, after national emergency was declared on March 13 [40].
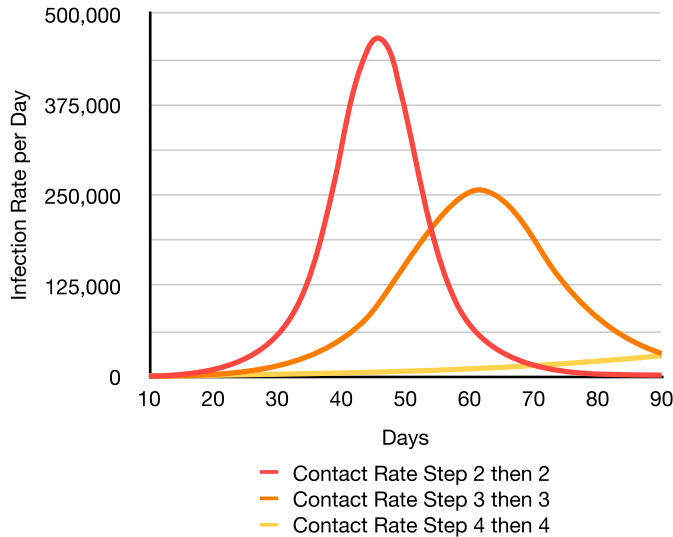
Fig. 2. Scenario 1: Infection rate over time—baseline assessment and verification. Three simulation runs shown with different reduction steps of the contact rate that drives the infections. The varying peaks of the simulation runs result from the slower disease spread, which also lowers the peak infection rate.
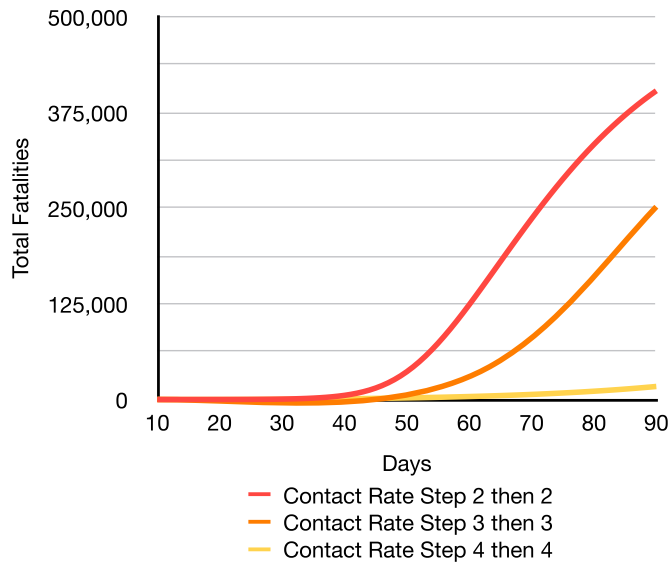


Fig. 3. Scenario 1: Fatalities over time–baseline assessment and verification. Three scenarios shown with different reduction steps of the contact rate that drives the infections. Reduction steps were introduced on day 16, and subsequently on day 21, respectively.

Hence, the scenario below was constructed to evaluate these two policies' effects. In a first run, the two dates were utilized to introduce contact rate reduction steps. Figs. 2 and 3 show the results for a period of 90 days, corresponding March 1 through the end of May.

Since there is a direct connection between the contact rate and the infection rate, as per the parameter $\beta$ described above, the contact rate steps simulated in Scenario 1 directly drive the different infection rates. Contact and exposure reductions are caused by measures and restrictions put into place or even people losing their jobs entirely in some cases. Then, due to the reduction in contacts, the average contact rate decreases, which in conjunction with the infectivity and the levels of
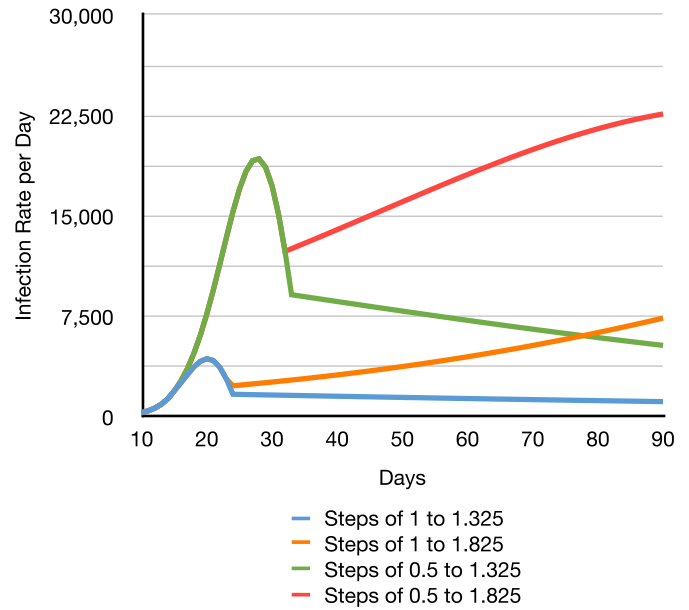


Fig. 4. Scenario 2: Infection rate over time—baseline assessment and verification. Four simulation runs shown with gradual contact rate reductions.

the susceptible stock, defines the infection rate at each time step/day. In addition, behavioral changes are another factor that affects and lowers the number of contacts that people have. For instance, if people try to consciously stay away from each other and avoid crowds, the average contact rate drops as well.

Figs. 2 and 3 show that the run of Scenario 1 "Contact Rate Step 2 then 2" does not result in a lasting reduction of the infection rate over time, and the fatalities still keep increasing constantly, despite the implemented measures. Hence, the measures of 2 steps of 2 do not show an impact significant enough to flatten the curve. Compared to the run "Contact Rate Step 4 then 4" for example, the total fatalities at the end of the simulation run is over 1300% higher for the run with steps of three and over 2200% higher for the run with steps of two. These effects are due to the fact that the reductions are not significant enough to have a helpful impact, and thus ultimately result in devastating fatality numbers.

### B. Scenario 2—Gradual Social Distancing and Closures

Scenario 2 evaluates the effects of gradually reduced contact rates over several days. The rates decrease over time until they reach a limit, which is more realistic since people adjust to new circumstances and in this case, to regulations, gradually over time. Thus, the starting point of the previous scenario was used to introduce gradual contact rate reductions.

The blue line in Fig. 4 shows the impact and resulting infection rate per day, for a reduction of one for the contact rate after day 16, for nine consecutive days until the rate reaches 1.325. Such reductions were cross-referenced with available mobility data [39] and showed that the parameters represent recorded behavior.

The resulting data show that the run with the steps of 0.5 down to 1.325 is closest to reality and approaches the fatality number reported [33], therefore verifying the model. The gradual reduction of the contact rate leads to a peak in the
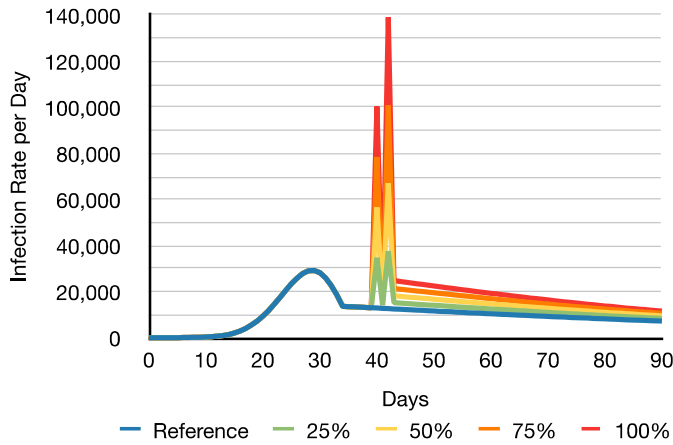
Fig. 5. Scenario 3: Isolated increases in contact rate—infection rate showing the two peaks for the contact rate increases on day 40 and 42 with the latter ones being higher and amplified by the first one. Day 43 and later show the infection rates which are permanently increased, caused by the prior spike.

infection rate, which introduces a downswing and successive upswing with a lower gradient. Hence, the gradual reduction of the contact rate is effective in controlling the epidemic and can hedge the upswing (Fig. 4).

## VI. EASTER AND PASSOVER HOLIDAY BLIP

The assessed baseline scenarios show changes that are linear or follow a gradient. This is not the case in reality because even a singular or short-term relaxation in rules or temporary exemptions can cause devastating results and major changes to the contact rate for a brief period [41].

At the time of the first simulations (April 2020), Easter and other religious holidays were happening. During such holidays, people tend to congregate, attend religious gatherings such as masses, and visit family members. After a prolonged period of solitude, the perceived need and yearning for such close contacts increases understandably and there have already been reports of planned gatherings [42]. In addition, significantly increased mobility was measured in Germany [39], [43], and people (including two of the authors) have witnessed Good Friday gatherings in New Jersey and New York, for example.

These phenomena suggest scenarios involving relaxation or defiance of the recommended measures. Hence, this section looks at possibilities in two scenarios to estimate the implications of such defiance in order to enable a prediction regarding the outcome. Scenario 3 assesses the possibility of increased contact rates on single-event occasions, and Scenario 4 evaluates short periods of increases. As a basis for the scenarios, the trajectory closest to reality of Scenario 2 is utilized.

### A. Scenario 3—Isolated Increases in Contact Rate

To utilize a real-life example, the run from Scenario 2 was simulated with the steps of 0.5 down to 1.325, and two short increases in contact rate for Good Friday and Easter Sunday implemented. To simulate various magnitude of increases, four runs were conducted with increments of 25% contact rate
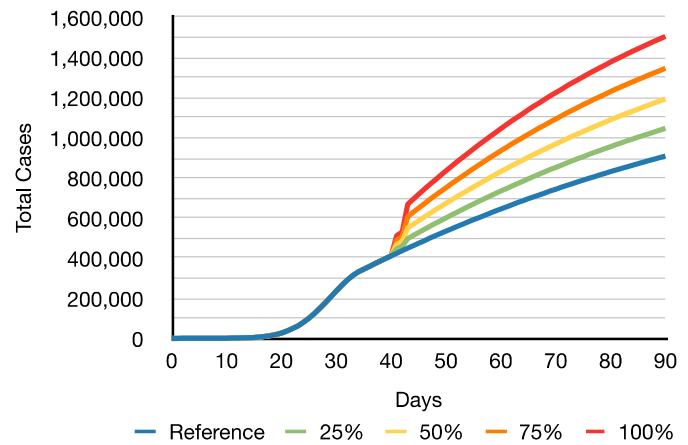


Fig. 6. Scenario 3: Isolated increases in contact rate—total cases showing the effects of the two peaks on day 40 and 42 and the impact of the permanently increased infection rates in form of higher gradients for the simulated runs.
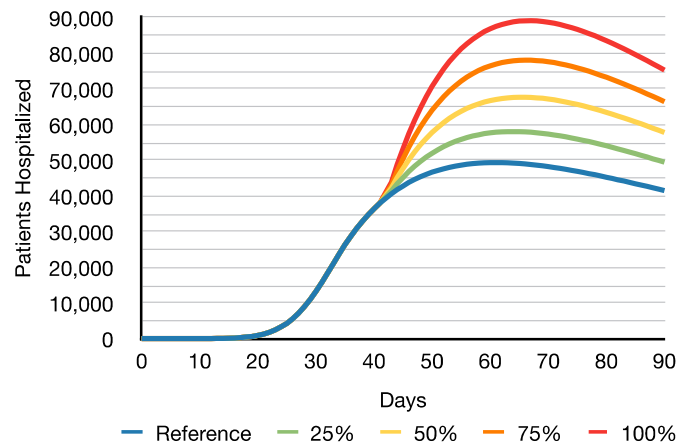


Fig. 7. Scenario 3: Isolated increases in contact rate—hospitalizations showing how many people require hospitalization for Scenario 3 each day after the delay of the incubation. This represents the required hospitalizations, which may exceed the real capacities of the hospitals, and therefore cause shortage and possibly even triage situations as described. The predicted hospitalization numbers allow for estimation of necessary resources for the simulated area.

increase, yielding the last run as a return back to the contact rate $c_0$ of 10.325. The results are depicted in Figs. 5–8.

The figures show that a return to the contact rates of a "normal" state can increase the infection rates temporarily by 980% as the first day with increased contact rates amplifies the second one. This amplification is due to the time between those two dates being too short for the measures to fight back the upswing. Therefore, the two increases yield hundreds of thousands of new infections and also double the number of hospitalized patients. In addition, in the long run, these short increases in contact rates have detrimental impacts when it comes to the fatality numbers. In the worst case run, the fatality numbers increase by 60% after 90 days, not taking into consideration that hospitals may be overloaded and forced into triage procedure where limited resources have to be allocated and decisions made concerning which patients can be admitted.
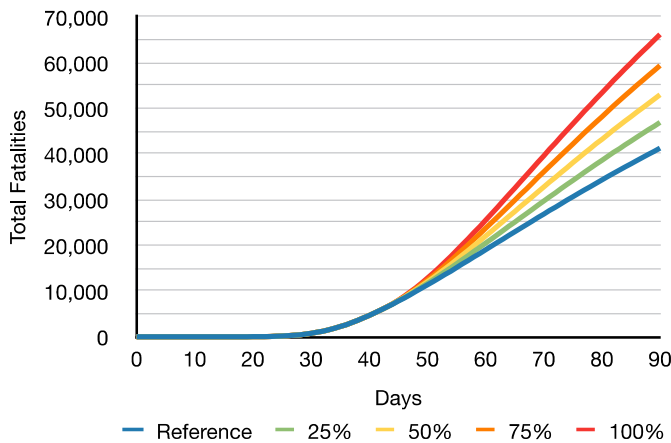
Fig. 8. Scenario 3: Isolated increases in contact rate—fatalities that show the increasing deaths over time, with the different gradients based on the height of the peaks shown in the infection rates.
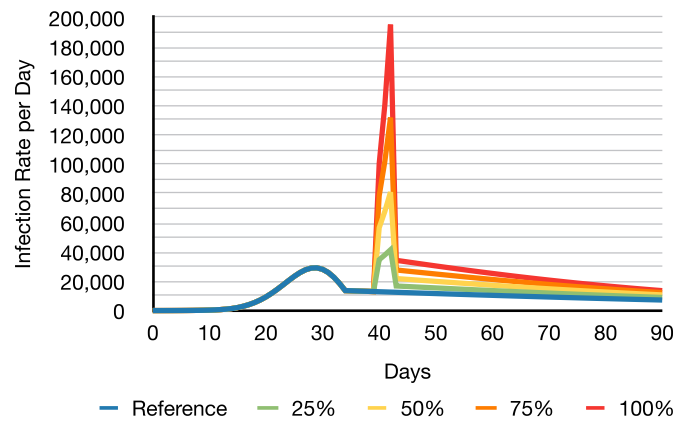


Fig. 9. Scenario 4: Temporarily sustained increase in contact rate—infection rate per day showing the constantly increasing rates from day 40 through 42. The first two days each amplify the subsequent one, which exacerbates the effect after the subsidence, since the reaming infection rate is even more elevated than the one in Scenario 3.



Fig. 10. Scenario 4: Temporarily sustained increase in contact rate—total cases showing the effects of the rapidly increasing infections from day 40 through 43 and the impact of the permanently increased infection rates over time, in form of higher gradients for the simulated runs.
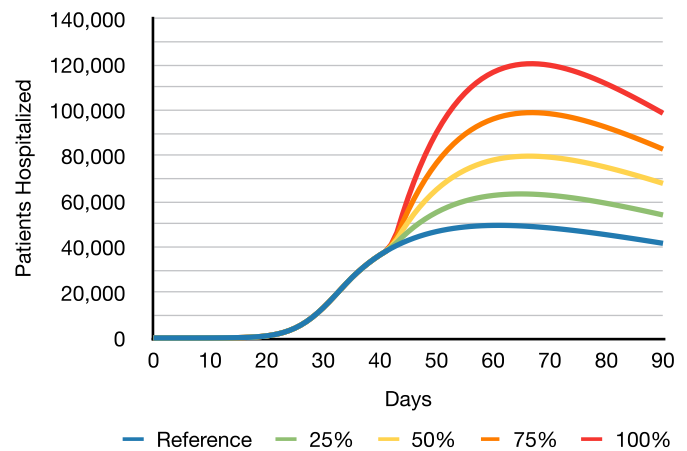


Fig. 11. Scenario 4: Temporarily sustained increase in contact rate—hospitalizations showing even higher numbers of people requiring hospitalization after the delay of the incubation compared to Scenario 3. This results in even higher stress and loads for the hospitals and other infrastructure, and presents an increased threat of collapse.

Overall, this scenario shows that singular increases already can have detrimental impacts and make the difference between healthcare infrastructure being overloaded or able to handle the demand. In addition, the simulation provides the numbers and results right away, whereas in reality incubation time may lead to a delay, and thus the individuals infected over Easter could affect the medical infrastructure one to two weeks later.

With these aspects in mind, the last scenario assesses the worst possible option, a temporarily sustained increase that is not isolated, but sustained for a certain period of time.

### B. Scenario 4—Temporarily Sustained Increase in Contact Rate

The above scenario assessed and illustrated short singular increases, which may repeatedly happen for future holidays. The last scenario assesses a constant increase over Easter weekend, for example, if people would spend multiple days with family or at other gatherings, which is not uncommon.

For instance, if a family visit were combined with a stay at someone else's home, a sustained exposure and contact rate increase is the result.

In order to simulate various magnitudes of contact rate increases, four runs were conducted with differences of 25% yielding the past run as a return all the way to $c_0$ of 10.325 for three days (Good Friday through Easter Sunday). The results are depicted in Figs. 9–12, and discussed thereinafter. Fig. 13 shows the hospitalizations over 180 days for demonstration and reference purposes.

The figures resulting from the last scenario show that the effects are partially as to be expected based on Scenario 3 since the infection rate steadily rises with every day the increase persists. Thus, the impact that the measures have when they are back in effect is also reduced. For example, for the infection rate on the first day after the increased period, the numbers are between 10% and 40% higher than they were in the respective runs of Scenario 3. This means that
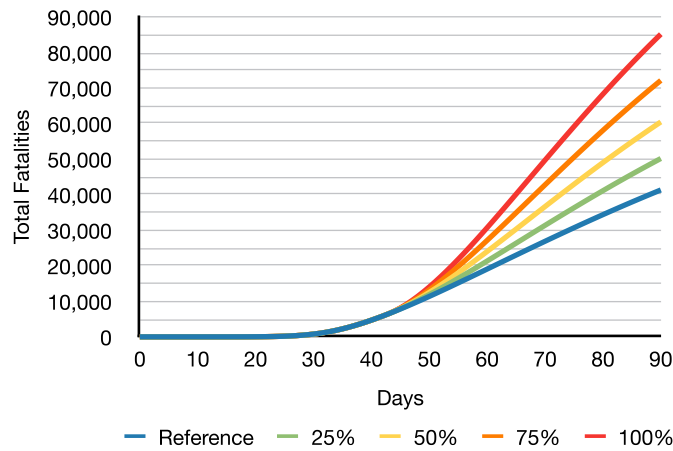
Fig. 12. Scenario 4: Temporarily sustained increase in contact rate—fatalities over time showing the even higher numbers and gradients compared to Scenario 3 due to the sustained temporarily sustained increase in contact rates.
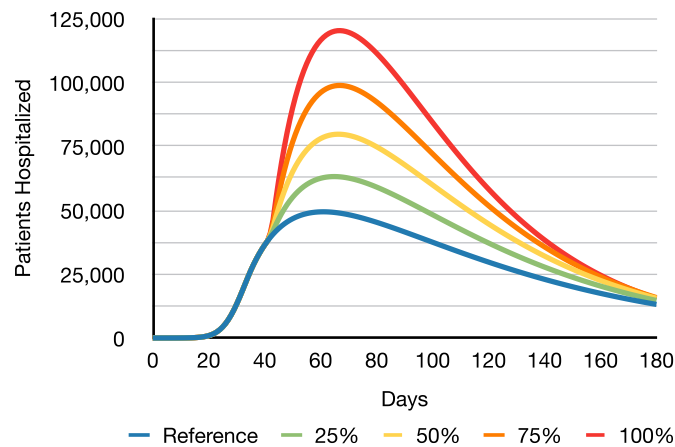


Fig. 13. Scenario 4: Temporarily sustained increase in contact rate—hospitalizations over 180 days showing the continued decline in required resources. This is dependent on a constant adherence to the measures and cannot be achieved with further deviations.

each day the increase persists has permanent effects on the infection rates even once the contact rate goes back down. This permanent influence can have extreme ripple effects for the hospitalization and fatality numbers as shown in Figs. 11 and 12: the hospitalization numbers are between 8.9% and 34.9% higher than the respective runs of Scenario 3, and between 29% and 146% higher than the reference run; the fatality numbers are between 6.8% and 28.6% higher than the respective runs of Scenario 3, and between 21.4% and 106% higher than the reference run over 90 days.

It can be observed that a temporarily sustained increase in contact rate, not only increases the number of patients and therefore causes effects over the time of its existence, but it permanently increases the total spread and numbers of patients. This allows for two conclusions: one, it is imperative to prevent such increases at all costs and two, if they are inevitable, they must be kept as low and short as possible, in order to minimize the permanent impact they have, and reduce their overall effects in the long run.

## VII. DISCUSSION

The previous sections and simulation results show that the spread of COVID-19 is dynamic and complex as emergent phenomena, disproportionate effects, and nonlinear behaviors have been discovered in the scenarios. Even with the social distancing and isolation measures mandated in April 2020, short increase and returns to "normal" contact rates can have detrimental outcomes that cause irreversible increases in the number of infections and patients, as the permanently increased numbers in Scenarios 3 and 4 show (see different runs depicted in Figs. 5 and 9, for example).

In numbers, the simulations have shown that even temporary contact rate spikes permanently increase infection rates by as much as 40% and even higher surges, such as a return to "normal" and therefore 100% increase of the contact rate would increase the infection rate temporarily by over 1800% (Fig. 9). These effects ripple through the system and impact hospitalizations and ultimately fatalities, increasing the former by as much as 146% (Fig. 11) at the peak, and the latter by as much as 106% (Fig. 12) in the worst case scenario compared to the references run without any contact increases.

Given that increases of 25% in contact rate seem to be most likely according to the data seen in Germany for the Easter weekend [39], [43], the simulations show the following increases after 90 days (compared to the realistic reference run) for a temporary 25% surge in contact rate around the holidays: the total number of infections grew by 215 880 (Fig. 10), the maximum of required hospitalizations increased to 63 063 (Fig. 11), and the total climb in fatalities was 8844, accumulated over the 90 days (Fig. 12). For the 50% surge, the total number of cases increased by 461 090 (Fig. 10), the maximum number of required hospitalizations increased to 79 733 (Fig. 11), and the total number of fatalities climbed by 19 125 over 90 days in NYC (Fig. 12).

All in all, the numbers and scenarios demonstrate that contact rate increases of any kind should be prevented at all costs in order to not permanently impact the progress of the pandemic and its containment. As the scenarios show (see Fig. 12, for example) no matter how small the increase is, and even if it is just temporary, it will have lasting and irreversible effects in the long run, such as increased total fatalities or respectively higher hospitalization number peaks. Such effects can be detrimental and due to their irreversible nature, the only way to address them effectively is proactively.

If increases cannot be prevented, it is imperative to keep them as short as feasible, and if necessary separate the peaks as much as possible to allow for regulation and mitigation in between, as the simulation scenarios have shown that sustained increases have more grave effects than separated spikes. For example, the worst case run of Scenario 4 shows an over 76% higher fatality count increase at the end of the simulation run, despite only adding one additional day with the same contact rate spike to form three consecutive days instead of two separated ones. Furthermore, other mitigation strategies such as stricter regulations could be a possibility to mitigate already occurred singular increases to compensate and address the irreversible effects moving forward.
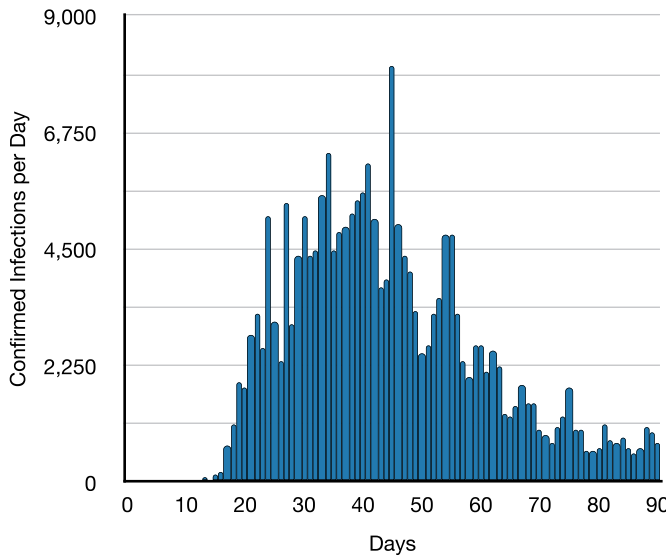
Fig. 14.   Confirmed cases in New York state based on official reports [37].

The simulations show the implications and results of increased infection rates before they might occur. This allows for the assessment of possible changes without having to reactively await their development, which is important when it comes to the hospitalization rates, for instance, as increased infection rates for even short periods, such as the described holiday blip, can significantly impact the hospitals and reduce free capacity in reality. Capacity worst case scenarios could force some hospitals into triage when they run out of beds. For example, Scenario 4 shows a peak hospitalization count increase of 146% for the most extreme simulation run (see "100%" in Fig. 13) over the reference, which would exceed all available hospital beds in NYC [44]. In addition, said beds are for all patients, not only COVID-19 related ones. With such numbers, local and even widespread problems seem likely.

Nevertheless, the analysis above was performed prior to observing any outcomes of social distancing or the impact of the mentioned holidays. Now that the actual data are available, they can be compared to the stated predictions. Fig. 14 shows the confirmed cases per day for the state of New York.

Fig. 14 shows an initial peak in infections 33 days after March 1 (day 0 of the simulation), with 6333 new confirmed infections. Comparing this first peak of Fig. 14 to the results of the simulation (Fig. 4) shows that the initial peak of the confirmed cases lies between the possibilities for different social distancing scenario. Fig. 14 thus matches the pattern of gradually increasing social distancing measures and further confirms the structure of the simulation model.

Furthermore, there are three very noticeable spikes in the confirmed cases after the first peak in Fig. 14: on days 38–42, 45, and 54 with 55. The model allowed the prediction of spikes between days 38 and 42 due to the Easter and Passover holidays. Thus, it is possible that the second spike in Fig. 14 is due to the holidays. If there was a greater delay from initial contacts to confirmed infections than modeled, the much higher spike on day 45 could be due to the holidays as well.

It has to be noted nevertheless, that the data shown in Fig. 14 do have a fair amount of noise, so even though there

appears to be spikes due to the holidays, it is possible that the actual effects are drowned by that noise. Such noise is also likely caused by reporting delays and the fact that it is difficult to obtain correct numbers for every single day. It is, for example, likely that numbers are not reported correctly over the weekends due to some offices being closed. Numbers would then be reported after the weekend, which could cause further distortion and inflated numbers at the beginning of the week.

The final interesting detail about the confirmed numbers in Fig. 14 is the oscillations in the spikes. These swings are potentially created by one spike that causes more infections, which results in another subsequent, and so forth. Such a connection has been shown by the simulations (Fig. 9). As described in the prior paragraphs of this discussion, consecutive days with increased contact rates result in disproportionately high increases in the respective numbers.

## VIII. CONCLUSION

The presented framework and results show that the chosen approach and developed framework can predict the results of certain influences on the progress of the pandemic. Since the model is built dynamically and shows complexity, it can show the emergent behaviors that may not be visible by assessment of linear connections of the formulas and underlying structures. As the case studies above show, some influences and outcomes have already been seen that are disproportionate in their effect.

The model allows for the testing of important and or critical scenarios. Since emergence can occur at unexpected times, and therefore inherits an element of surprise, testing various scenarios for their stability can also be crucial for regulatory measures. For instance, margin cases and extreme capacity scenarios could be simulated in order to determine the boundaries of the system and its behavior close to these areas. Such testing can then support informed decisions that regulate and guide the real entities and systems to prevent critical developments entirely.

A framework and model, such as the one presented, provide crucial opportunities and benefits, as it does not only copy and try to reproduce progress, but instead dynamically simulates it with high flexibility and immediate display of emergent behaviors.

In addition, the model provides a unique adaptability as it can implement and therefore respond to minute as well as substantial changes on the input side. Many scenarios can be evaluated and assessed regarding their effects. This adaptability is also key when it comes to long-term predictions as with increased durations, the opportunities and amount of potential influencing factors increases. Thus, having the possibility and capability to include and account for changes in an adaptable way is an important advantage.

Overall, the designed model and simulations allow for a realistic representation and predictive possibilities, as well as future applications. Extensions and continued development of the simulation and model are planned and being worked on in order to achieve an even more accurate and realistic framework that can help to understand, anticipate, and therefore potentially reduce fear and uncertainty for pandemic times when many people are questioning the fundamental necessities and pillars of everyday life.

## References

[1] World Health Organization. *What is a Pandemic*. Accessed: Apr. 10, 2020. [Online]. Available: https://who.int/csr/disease/swineflu/frequently_asked_questions/pandemic/en/

[2] World Health Organization. *Coronavirus Disease (COVID-19) Pandemic*. Accessed: Apr. 10, 2020. [Online]. Available: https://who.int/emergencies/diseases/novel-coronavirus-2019

[3] Y. Shu and J. McCauley, "GISAID: Global initiative on sharing all influenza data–from vision to reality," *Eurosurveillance*, vol. 22, no. 13, p. 30494, Mar. 2017, doi: 10.2807/1560-7917.ES.2017.22.13.30494.

[4] A. Wu *et al.*, "Genome composition and divergence of the novel coronavirus (2019-nCoV) originating in China," *Cell Host Microbe*, vol. 27, no. 3, pp. 325–328, Mar. 2020, doi: 10.1016/j.chom.2020.02.001.

[5] K. Ćosić, S Popovic, M. Šarlija, I. Kesedžic, and T. Jovanovic, "Artificial intelligence in prediction of mental health disorders induced by the COVID-19 pandemic among health care workers," *Croatian Med. J.*, vol. 61, no. 3, pp. 279–288, Jun. 2020, doi: 10.3325/cmj.2020.61.279.

[6] S. Lalmuanawma, J. Hussain, and L. Chhakchhuak, "Applications of machine learning and artificial intelligence for COVID-19 (SARS-CoV-2) pandemic: A review," *Chaos, Solitons Fractals*, vol. 139, Oct. 2020, Art. no. 110059, doi: 10.1016/j.chaos.2020.110059.

[7] G. Pinter, I. Felde, A. Mosavi, P. Ghamisi, and R. Gloaguen, "COVID-19 pandemic prediction for Hungary; A hybrid machine learning approach," *Mathematics*, vol. 8, p. 890, Dec. 2020.

[8] R. Vaishya, M. Javaid, I. H. Khan, and A. Haleem, "Artificial intelligence (AI) applications for COVID-19 pandemic," *Diabetes Metabolic Syndrome, Clin. Res. Rev.*, vol. 14, no. 4, pp. 337–339, Jul. 2020, doi: 10.1016/j.dsx.2020.04.012.

[9] K. Pacheco-Barrios, A. Cardenas-Rojas, S. Giannoni-Luza, and F. Fregni, "COVID-19 pandemic and Farr's law: A global comparison and prediction of outbreak acceleration and deceleration rates," *PLoS ONE*, vol. 15, no. 9, Sep. 2020, Art. no. e0239175, doi: 10.1371/journal.pone.0239175.

[10] S. Rath, A. Tripathy, and A. R. Tripathy, "Prediction of new active cases of coronavirus disease (COVID-19) pandemic using multiple linear regression model," *Diabetes Metabolic Syndrome, Clin. Res. Rev.*, vol. 14, no. 5, pp. 1467–1474, Sep. 2020, doi: 10.1016/j.dsx.2020.07.045.

[11] R. K. Singh *et al.*, "Prediction of the COVID-19 pandemic for the top 15 affected countries: Advanced autoregressive integrated moving average (ARIMA) model," *JMIR Public Health Surveill.*, vol. 6, no. 2, May 2020, Art. no. e19115, doi: 10.2196/19115.

[12] A. Singhal, P. Singh, B. Lall, and S. D. Joshi, "Modeling and prediction of COVID-19 pandemic using Gaussian mixture model," *Chaos, Solitons Fractals*, vol. 138, Sep. 2020, Art. no. 110023, doi: 10.1016/j.chaos.2020.110023.

[13] I. Ciufolini and A. Paolozzi, "Mathematical prediction of the time evolution of the COVID-19 pandemic in italy by a gauss error function and Monte Carlo simulations," *Eur. Phys. J. Plus*, vol. 135, no. 4, p. 355, Apr. 2020, doi: 10.1140/epjp/s13360-020-00383-y.

[14] K. Y. Ng and M. M. Gui, "COVID-19: Development of a robust mathematical model and simulation package with consideration for ageing population and time delay for control action and resusceptibility," *Phys. D, Nonlinear Phenomena*, vol. 411, Oct. 2020, Art. no. 132599, doi: 10.1016/.j.physd.2020.132599.

[15] O. de Weck, D. Krob, L. Lefei, P. C. Lui, A. Rauzy, and X. Zhang, "Handling the COVID-19 crisis: Toward an agile model-based systems approach," *Syst. Eng.*, vol. 23, pp. 656–670, Aug. 2020, doi: 10.1002/sys.21557.

[16] M. Casares and H. Khan, "A dynamic model of COVID-19: Contagion and implications of isolation enforcement," Carleton Univ., Ottawa, ON, Canada, Charlton Econ. Working Papers 20-02, May 2020. [Online]. Available: https://carleton.ca/economics/wp-content/uploads/cewp20-02.pdf

[17] J. Huang *et al.*, "Global prediction system for COVID-19 pandemic," *Sci. Bull.*, vol. 65, no. 22, pp. 1884–1887, Nov. 2020, doi: 10.1016/j.scib.2020.08.002.

[18] W. O. Kermack and A. G. McKendrick, "A contribution to the mathematical theory of epidemics," *Proc. R. Soc. Lond. A, Math. Phys. Sci.*, vol. 115, no. 772, pp. 700–721, 1927, doi: 10.1098/rspa.1927.0118.

[19] D. S. Jones, M. Plank, and B. D. Sleeman, *Differential Equations and Mathematical Biology*, 2nd ed. London, U.K.: Chapman & Hall, 2009.

[20] *Interim Clinical Guidance for Management of Patients with Confirmed Coronavirus Disease (COVID-19)*. Accessed: Oct. 31, 2020. [Online]. Available: https://cdc.gov/coronavirus/2019-ncov/hcp/clinical-guidance-management-patients.html

[21] *Duration of Isolation and Precautions for Adults with COVID-19*. Accessed: Oct. 31, 2020. [Online]. Available: https://cdc.gov/coronavirus/2019-ncov/hcp/duration-isolation.html

[22] S. A. Lauer *et al.*, "The incubation period of coronavirus disease 2019 (COVID-19) from publicly reported confirmed cases: Estimation and application," *Ann. Internal Med.*, vol. 172, no. 9, pp. 577–582, 2020, doi: 10.7326/M20-0504.

[23] N. Linton *et al.*, "Incubation period and other epidemiological characteristics of 2019 novel coronavirus infections with right truncation: A statistical analysis of publicly available case data," *J. Clin. Med.*, vol. 9, no. 2, p. 538, Feb. 2020, doi: 10.3390/jcm9020538.

[24] E. M. Rees *et al.*, "COVID-19 length of hospital stay: A systematic review and data synthesis," *BMC Med.*, vol. 18, no. 1, p. 270, Dec. 2020, doi: 10.1186/s12916-020-01726-3.

[25] J. J. A. van Kampen *et al.*, "Duration and key determinants of infectious virus shedding in hospitalized patients with coronavirus disease-2019 (COVID-19)," *Nature Commun.*, vol. 12, no. 1, p. 267, 2021, doi: 10.1038/s41467-020-20568-4.

[26] *Vensim Software*. Accessed: Apr. 1, 2020. [Online]. Available: http://vensim.com

[27] A. Maria, "Introduction to modeling and simulation," in *Proc. 29th Conf. Winter Simulation*, Atlanta, GA, USA, 1997, pp. 7–13.

[28] *Population—Current and Projected Populations*. Accessed: Apr. 11, 2020. [Online]. Available: https://1.nyc.gov/site/planning/planning-level/nyc-population/current-future-populations.page

[29] S. L. Chang, N. Harding, C. Zachreson, O. M. Cliff, and M. Prokopenko. *Modeling Transmission and Control of the COVID-19 Pandemic in Australia*. Accessed: Apr. 11, 2020. [Online]. Available: https://arxiv.org/abs/2003.10218

[30] A. M. Otto. *COVID-19 Update: Transmission 5% or Less Among Close Contacts*. Accessed: Apr. 11, 2020. [Online]. Available: https://the-hospitalist.org/hospitalist/article/218769/coronavirus-updates/covid-19-update-transmission-5-or-less-among-close

[31] H. T. Banks and C. Castillo-Chavez, *Bioterrorism: Mathematical Modeling Applications in Homeland Security*. Philadelphia, PA, USA: Society for Industrial and Applied Mathematics, 2003.

[32] *Means of Transportation to Work by Selected Characteristics*. Accessed: Apr. 11, 2020. [Online]. Available: https://data.census.gov/cedsci/table?q=S0802&tid=ACSST1Y2018.S0802

[33] *COVID-19: Data*. Accessed: Apr. 11, 2020. [Online]. Available: https://1.nyc.gov/site/doh/covid/covid-19-data.page

[34] Y. Bai *et al.*, "Presumed asymptomatic carrier transmission of COVID-19," *JAMA*, vol. 323, no. 14, p. 1406, Apr. 2020, doi: 10.1001/jama.2020.2565.

[35] A. R. Tuite, V. Ng, E. Rees, and D. Fisman, "Estimation of COVID-19 outbreak size in Italy based on international case exportations," *medRxiv*, 2020, Art. no. 2020.03.02.20030049, doi: 10.1101/2020.03.02.20030049.

[36] CNBC. *The Total Number of Italian Coronavirus Cases Could be '10 Times Higher' Than Known Tally, According to One Official* Accessed: Apr. 11, 2020. [Online]. Available: https://cnbc.com/2020/03/24/italian-coronavirus-cases-seen-10-times-higher-than-official-tally.html

[37] The New York Times. *Coronavirus (COVID-19) Data in the United States*. Accessed: Jun. 1, 2020. [Online]. Available: https://github.com/nytimes/covid-19-data

[38] Centers for Disease Control Prevention. *Births and Natality*. Accessed: Oct. 31, 2020. [Online]. Available: https://cdc.gov/nchs/fastats/births.htm

[39] Apple. *COVID-19—Mobility Trends Reports*. Accessed: Apr. 14, 2020. [Online]. Available: https://apple.com/ covid19/mobility

[40] NBC Universal. *What's Closed What's Mandatory How Tri-State COVID-19 Action Affects Daily Life*. Accessed: Apr. 11, 2020. [Online]. Available: https://nbcnewyork.com/news/coronavirus/everything-tri-state-gov-officials-are-doing-to-control-spread-and-ease-concerns-of-covid-19/2314762/

[41] W. P. London and J. A. Yorke, "Recurrent outbreaks of measles, chickenpox and mumps: I. Seasonal variation in contact rates," *Amer. J. Epidemiol.*, vol. 98, no. 6, pp. 453–468, 1973, doi: 10.1093/oxfordjournals.aje.a121575.

[42] G. Hauck. *States are Restricting Easter Gatherings Amid COVID-19. Churches and Lawmakers are Pushing Back*. Accessed: Apr. 11, 2020. [Online]. Available: https://usatoday.com/story/news/nation/2020/04/11/coronavirus-easter-kansas-kentucky-restrict-religious-gatherings-church/2975593001/

[43] H. Dambeck. *Deutsche Sind Immer Mehr Unterwegs*. Accessed: Apr. 14, 2020. [Online]. Available: https://spiegel.de/panorama/corona-lockdown-deutsche-sind-immer-mehr-unterwegs-a-c8a6b940-600d-47c5-bf40-2ce4c26b9a7a

[44] J. Goldstein and B. M. Rosenthal. *Coronavirus in N.Y.: Will a Surge in Patients Overwhelm Hospitals*. Accessed: Dec. 18, 2020. [Online]. Available: https://www.nytimes.com/2020/03/14/nyregion/coronavirus-nyc-hospitals.html